STIFFNESS, FORCE, AND SARCOMERE SHORTENING DURING A TWITCH IN FROG SEMITENDINOSUS MUSCLE BUNDLES

MARK SCHOENBERG
Laboratory of Physical Biology, National Institute of Arthritis, Diabetes, and Digestive and Kidney Diseases, National Institutes of Health, Bethesda, Maryland 20205

JAY B. WELLS
Laboratory of Biophysics (IRP), National Institute of Neurological and Communicative Disorders and Stroke, National Institutes of Health, and the Marine Biological Laboratory, Woods Hole, Massachusetts 02543

ABSTRACT The time course of force and stiffness during a twitch was determined at 6 and 26°C in frog semitendinosus muscle bundles using the transmission time technique of Schoenberg, M., J. B. Wells, and R. J. Podolsky, 1974, *J. Gen. Physiol.* 64:623–642. Sarcomere shortening due to series compliance was also measured using a laser light diffraction technique. Following stimulation, stiffness developed more rapidly than force, but had a slower time course than published Ca^{2+} transients determined from light signals using Ca^{2+} sensitive dyes (Baylor, S. M., W. K. Chandler, and M. W. Marshall, 1982, *J. Physiol.* (*Lond.*). 331:139–177). Stiffness (S) did not reach its tetanic value during a twitch at 6 or 26°C, although at 6°C, it approached close to this value with $S_{twitch}/S_{tetanus} = 0.82 \pm 0.07$ (± SEM). During relaxation, force fell more rapidly than stiffness both for a twitch and also a tetanus. Also in this paper, several of the assumptions inherent in using the transmission time technique for the measurement of stiffness are considered in detail.

INTRODUCTION

In twitch muscle fibers, application of an electrical shock to the membrane triggers a number of events that are believed necessary for force development. To learn more about the events occurring during the interval between stimulation and the appearance of force, it would be helpful to know the time course of an intermediate step, perhaps cross-bridge attachment. Since cross-bridge attachment cannot, at present, be measured directly, we measure, in this paper, the time course of stiffness development.

The exact relationship between cross-bridge attachment and muscle stiffness has not been firmly established. The finding that the increase in stiffness upon activation at different sarcomere lengths is roughly proportional to the degree of overlap between the thick and thin filaments (Ford et al., 1981) suggests a correspondence. In relaxed muscle the presence of "viscous" behavior (D. K. Hill, 1968; Ford et al., 1977) suggests that the correspondence may not always be exact. We used the transmission time technique for the measurement of muscle stiffness (Schoenberg et al., 1974). This technique measures stiffness by recording the transmission time for a small mechanical disturbance to propagate along the length of the muscle. As we have pointed out (Schoenberg et al., 1974), it has the advantage of having an extremely short measurement time so that it causes little perturbation to the preparation during the time of measurement. Some of the difficulties of applying the technique are evaluated more fully in the current manuscript.

We found that although the apparent stiffness measured in this way develops more rapidly than force, its development is not so rapid as the inward spread of activation (Gonzalez-Serratos, 1971), or the apparent rise in intracellular Ca^{2+} in single fibers following electrical stimulation (Blinks et al., 1978; Baylor et al., 1982). The internal muscle sarcomere shortening was also measured, using light diffraction, and the relationship between this and the lag between stiffness and force is discussed.

METHODS

Preparation

Fibers from the ventral head of the frog (*Rana pipiens*) semitendinosus muscle were dissected away until a bundle containing 20–50 fibers remained. The bundles were tied and mounted as described in Schoenberg et al. (1974) or by clamping the tendon at both ends, as close as possible to the origin of the muscle fibers. They were mounted in a quartz chamber having slotted Lucite ends. The slots were filled with silicon Dow 4 compound (Dow Corning Corp., Midland, MI) to make the chamber watertight and still allow the clamps to pass out the end of the chamber.

One clamp was mounted to the force transducer and the other to a loud speaker voice coil (see Fig. 1). The fibers were bathed in slowly flowing Ringer's solution, containing NaCl 115.5 mM, KCl 2.5 mM, $CaCl_2$ 1.8 mM, sodium phosphate buffer 3.11mM, tubocurarine chloride, 15 mg/l, at pH 7.0. Experiments were done either at 6°C or room temperature, 23–26°C. The muscle bundles were stimulated by passing 0.5–2.0 ms current pulses (Grass Instrument Co., Quincy, MA) across two 1-mm diam platinum electrodes that were along the length of the preparation on either side of it.

Measurement of Sarcomere Length

As the walls of the muscle chamber were constructed from microscope slides, it was possible to project a laser beam upon the muscle bundle from the front of the chamber and record a diffraction pattern in the rear. The average sarcomere length of the muscle bundle within the area of the 1.3 mm diam beam was determined from the separation of the zeroeth and first-order lines. (The chamber wall thickness and distance to the plane of measurement were such that the error due to refraction was small.) This determination correlated well with the average sarcomere length of the preparation as determined from microscopic measurements using a long working distance objective with a magnification of 50 (Leitz Wetzlar, Federal Republic of Germany).

To detect small changes in sarcomere length, the first-order diffraction line was focused, using a cylindrical lens, upon a light position detector (UDT-SC-10, United Detector Technology, Santa Monica, CA; see Fig. 2). To make the position signal insensitive to intensity, the difference signal from the UDT-device was electronically divided by a signal proportional to light intensity. When this was done, a 44% decrease in light intensity gave a spurious displacement signal of <1 nm/half sarcomere. The sensitivity (which was dependent upon the amount of background light scatter) was measured at each location along the fiber bundle and was usually ~30–50 mV for a displacement corresponding to a

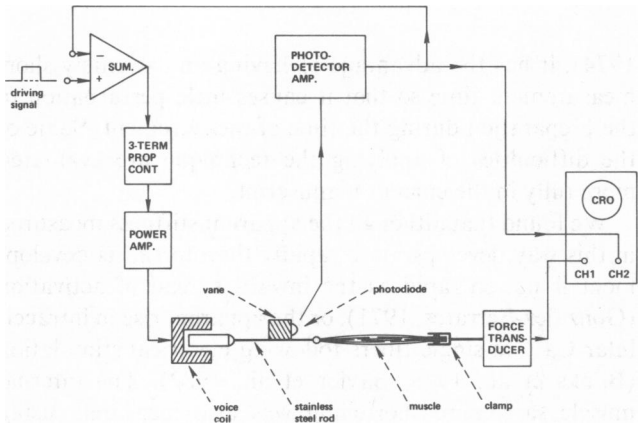

FIGURE 1 Schematic of experimental setup. *SUM* represents a group of high speed operation amplifiers, operated in the feedback mode, that compare the displacement signal from the displacement transducer (photodiode plus *PHOTODETECTOR AMP*) with the driving signal and produce an output signal proportional to the difference. This difference is fed through a three-term proportional controller (*3-TERM PROP CONT*), and then fed into a power amplifier (*POWER AMP*) that produces a current or voltage proportional to the modified difference signal that drives the voice coil, producing a displacement proportional to the driving signal. A vane, attached through a stainless steel rod to the moving voice coil, decreases the amount of light (from a light-emitting diode not shown) falling on a photodiode, which is the first stage of the displacement transducer. The displacement signal is then amplified and fed into an oscilloscope (*CRO*) along with the signal from the *FORCE TRANSDUCER*.

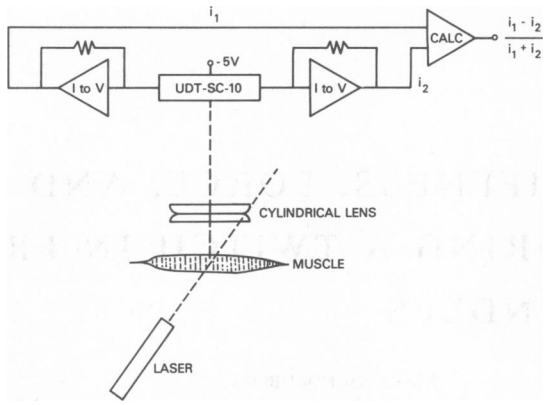

FIGURE 2 Schematic diagram of sarcomere length change recording apparatus. Laser light (632.8 nm) was projected upon the muscle and the first-order diffraction line was compressed, using two cylindrical lenses (combined focal length 25 mm) upon a United Detector Technology position sensitive light detector (*UDT-SC-10*). The detector was biased by −5 V. The currents from opposite poles of the *UDT-SC-10* were converted to voltage signals, i_1, and i_2, and were then fed through a series of operational amplifiers and a voltage divider (labeled *CALC*) so that a voltage signal equal to $(i_1 - i_2)/(i_1 + i_2)$ was generated. This was proportional to the position of the centroid of the light shining upon the detector.

sarcomere length change of 1 nm/half sarcomere. Both the noise and frequency response of the system depended upon the intensity of the incident light. With a 2 mW He-Ne laser (model 133, Spectra-Physics, Inc., Mountain View, CA) the noise level corresponded to a length change of 1 nm/half sarcomere and the response time of the system was ~1 ms. With a 10-mW laser (model HN-10, Jodon Engineering, Ann Arbor, MI), the noise level decreased to ~0.1 nm/half sarcomere and the response time decreased to ~30–100 μs. The device was linear (± 5%) for an excursion of ± 3 mm from the device center, corresponding to a movement of 50 nm/ half sarcomere.

Measurement of Transmission Time

The experimental apparatus for measuring stiffness using the transmission time technique was very similar to that reported earlier (compare Fig. 1 in this publication with Fig. 1 in Schoenberg et al., 1974). Several improvements were made. A smaller power operational amplifier with lower distortion was used (RCA HC2500, Radio Corporation of America, Somerville, NJ). The asymmetric notch filter was replaced by a three term proportional controller. This was a single operational amplifier that produced a signal that was the weighted sum of three terms; the error signal, its derivative, and its integral. The response of the speaker system was tuned by varying the weights of the three terms (De Barr, 1962). The speaker had a maximum velocity of 0.6 mm/ms and could accelerate to one-half this velocity in 0.15 ms. In the feedback mode, the stiffness of the system was such that a steady force of 200 kdyn produced a speaker displacement of <6 μm.

The displacement and force transducers were similar to those used previously. Modification of the displacement transducer yielded a device that was linear (± 2%) over 1.4 mm and had a sensitivity of 0.57 mV/μm. The noise equivalent was ± 0.5 μm peak-to-peak. Long term drift over 10 min was equivalent to 3.5 μm. The piezoelectric force transducer (model 209M, PCB Piezotronics, Buffalo, NY) had an unloaded natural frequency, >100 kHz. When loaded with the muscle clamp, this decreased to 25 kHz. Its compliance was $<3 \times 10^{-9}$ cm/kdyn and its sensitivity 5 mV/kdyn. The nonthermal drift (higher frequency) noise was equivalent to 40 dyn peak-to-peak. Since piezoelectric transducers are alternating current devices (the time constant of our transducer was nominally 10 s),

it was important to ascertain that relaxation of the force transducer was not a major factor in interpretation of the records. For a force signal in the shape of a half-cycle sine wave of 25-ms duration (mimicking a twitch at room temperature), the decrement in the magnitude of the force caused by transducer relaxation was <1%. For a half cycle of 300 ms (a time scale similar to a twitch at 6°C) the decrement was ~8%. For a half cycle of 1,400 ms, the decrement was still only 12%.

Reading the Records

For measurement of the transmission time, the fixed lag in the system that needed to be subtracted from the recorded delay times was 57 μs. This was determined by measuring the delay in force when the speaker was quickly displaced from abutting the force transducer (see Schoenberg et al., 1974). Fig. 3 shows several typical records and how the records were read. *A* and *B* show repeat transmission time measurements on the same bundle under identical conditions during the plateau of a tetanus. The precision of the repeat transmission time values, 55 μs for *A* and 59 μs for *B*, was typical so long as the force level was above ~0.1 P_o. Below that level, the signal-to-noise ratio was such that it became difficult to read the records with a precision of >20%. The reproducibility of the force records was ~3% in experiments like those shown in Fig. 4 (constant sarcomere length) and 15% in ones like those shown in Fig. 9 (variable sarcomere length). The larger variation in the latter case was most likely related to variability in reproducing sarcomere length.

RESULTS

Time Course of Stiffness and Force During A Twitch

Fig. 4 shows the development of stiffness and force in typical experiments during twitches at 6 and 26°C when the ends of the muscle preparation are held fixed. The preparation was stimulated with a single supramaximal shock at time zero and, with repeat maneuvers using the transmission time technique, stiffness and force were measured at different times following stimulation. The points in Fig. 4 were obtained in random order with a tetanic and resting control every 7–10 records. In Fig. 4, both relative force and relative stiffness are plotted as a fraction of the values obtained during the plateau of a tetanus. The relative stiffness was calculated as $(\tau_{P_o}/\tau)^2$ in accordance with Eq. 7 of Schoenberg et al. (1974), where τ_{P_o} is the transmission time during the plateau of a tetanus. Three regions of interest in Fig. 4 are discussed below: the rising phases of each curve, the peaks of the curves, and the falling phases.

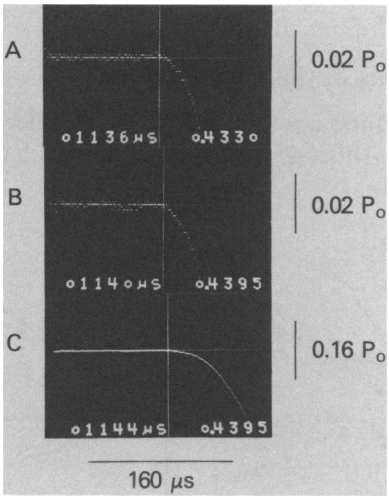

FIGURE 3 Measurement of transmission time. Original records showing force vs. time. Data were extracted from records such as *A* and *B*. At t = 1,024 μs, the driving voltage to the loudspeaker was applied. Since the fixed lag in the system was 57 μs, the transmission time τ was computed as $t' - 1{,}024 - 57$ μs, where t' was the time, chosen by eye, that the force record started to fall. This time is indicated by the cross-hairs and light-emitting-diode readout in the records shown, which come from a digital oscilloscope (model 1090, Nicolet Instrument Company, Madison, WI). *A* and *B* represent repeat measurements on one tetanized bundle. The precision represented by τ = 55 μs for *A* and 59 μs for *B* is typical. Record *C*, shows the same data as record *B* with the vertical scale sensitivity reduced eightfold. The apparent increase in t' illustrates that a decrease in force as large as eightfold could result in an apparent decrease in stiffness of ~12%. This effect, related to noise in the force trace, could be reduced by signal averaging.

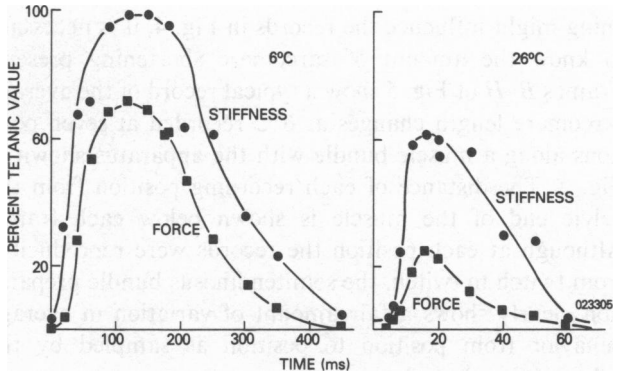

FIGURE 4 Force and stiffness following a single supramaximal shock at 6 and 26°C. Circles, (●), stiffness; squares (■), force. Stimulus at time zero. Values expressed as percent of tetanic value. Experiment 023305. P_o = 15.6 kdyn at 26°C; P_o = 12.0 kdyn at 6°C; length = 0.95 cm; mass = 6.4 mg. Sarcomere length = 2.2 μm.

Rising Phase: Relationship Between Stiffness and Force

From Fig. 4 it is clear that relative to the fully activated tetanic isometric state, force develops less rapidly than stiffness during the rising phase of the twitch. The same would be true under our conditions for the early rising phase of a tetanus since the initial portions of both experiments are identical. In the experiments of Fig. 4 the lag between stiffness and force at a force of P = 0.25 P_o is ~22 ms at 6°C and 6.5 ms at 26°C. In a total of eight experiments the average lag at 6°C was 19.3 ms (range 8–27 ms) and 5.1 ms (range, 4.2–6.5) at 26°C.

Sarcomere Shortening During the Rising Phase of a Twitch

Although the ends of the muscle bundle preparation were held fixed in the experiment of Fig. 4, it is known that under these conditions the muscle sarcomeres themselves are not isometric (Jewell and Wilkie, 1958; Cleworth and Edman, 1972). To assess to what extent sarcomere short-

ening might influence the records in Fig. 4, it is necessary to know the amount of sarcomere shortening present. Frames *B–H* of Fig. 5 show a typical record of the average sarcomere length changes at 6°C recorded at seven positions along a muscle bundle with the apparatus shown in Fig. 2. The distance of each recording position from the pelvic end of the muscle is shown below each frame. Although at each position the records were reproducible from twitch to twitch, the semitendinosus bundle preparation clearly shows a fair amount of variation in average behavior from position to position as sampled by the 1.3-mm diam laser beam.[1]

Although, this spatial variability of sarcomere shortening might be important when comparing the stiffness behavior of bundles and single fibers (see Kobayashi and Sugi, 1982), for purposes of calculating the effect of series compliance on the time course of force and stiffness, it is appropriate to ignore those regions of the muscle bundle that show lengthening and consider only those regions that show shortening (see footnote 3, Discussion). To illustrate the average apparent compliance in series with those areas of the muscle that shorten following stimulation, Fig. 6 *A* shows plots of sarcomere length vs. force during the rise of twitch tension for each record of Fig. 5. Fig. 6 *B* shows similar data from an experiment done at room temperature. The number next to each curve signifies the distance of each position in millimeters from the pelvic end of the muscle bundle. The dashed lines labeled *A* in Fig. 6 *A* and *C* in Fig. 6 *B* have a slope corresponding to a compliance with an $L_{1/2}$ of 0.04, where $L_{1/2}$ is defined as the fractional change in length accompanying a force change from $P = P_o$ to $P = 0.5\ P_o$. The dashed line labeled *B* corresponds to a compliance of $L_{1/2} = 0.015$. Considering only those locations showing significant shortening (i.e., curves labeled 2, 4, 6, and 8 in Fig. 6 *A* and 1.9, 3.8, and 9.5 in Fig. 6 *B*), it is seen that between $P = 0$ and $P = 0.1\ P_o$ the local shortening is about the same as it would be if a simple compliance of magnitude $L_{1/2} = 0.04$ were in series. Between $P = 0$ and $P = 0.8\ P_o$, the corresponding apparent compliance is $L_{1/2} = 0.015$. These values are important in evaluating the effect of compliance upon force and stiffness development. (See Discussion.)

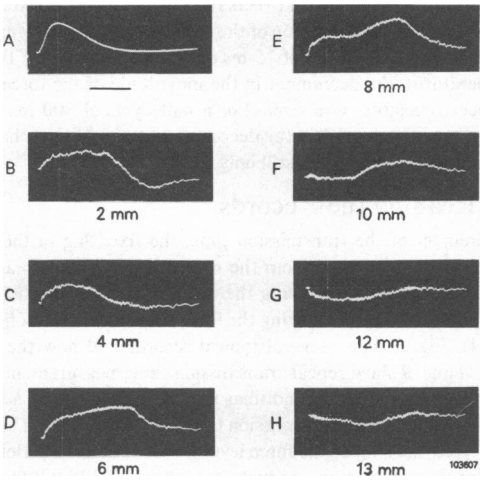

FIGURE 5 Typical sarcomere length changes during a twitch at 6°C. *A*, twitch force. *B–H* sarcomere length changes at different locations along bundle preparation. Horizontal axis, time. Horizontal bar under frame *A*, the time calibration for all the records, represents 200 ms. Numbers below each record show the distance from the pelvic end of the muscle at which the 1.3-mm laser beam was projected through the preparation. Vertical calibration bars to the right of each frame correspond to a length change of 44 nm/half-sarcomere, shortening upward. Peak force in frame *A* is 2.3 kdyn. Experiment 103607. P_o = 3.1 kdyn; mass = 3.9 mg; length = 1.5 cm. Resting sarcomere length during experiment, 2.4 μm. Temperature, 6.1° ± 0.2°C.

Peak of the Twitch

Neither stiffness nor force reached its tetanic value during the twitch. Although at 6°C, stiffness reached a fraction

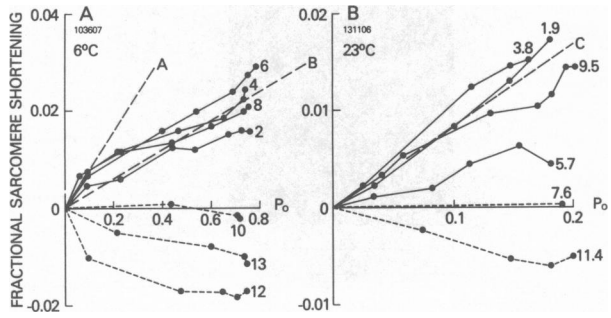

FIGURE 6 Typical records of sarcomere shortening vs. force during the rising phase of a twitch. *A*, 6°C. *B*, 23°C. *Abscissa*, force as a fraction of P_o. *Ordinate*, sarcomere shortening as a fraction of SL_o, resting sarcomere length. (+ 0.02 corresponds to a shortening of 22 nm/half sarcomere.) Numbers near each record are the distance in millimeters from the center of the 1.3-mm laser beam to the pelvic end of the muscle. Short dashed lines (---) show curves for those positions that lengthened or remained the same during contraction. Long dashed lines (– – –) labeled *A* and *C* show the expected shortening vs. force relationship if sarcomere shortening was due simply to a linear compliance of $L_{1/2} = 0.04$ in series. The long dashed line (– – –) labeled *B* shows the same for a compliance of $L_{1/2} = 0.015$. Data at 6°C was obtained from the same experiment as Fig. 5; data at 23°C was from experiment 131106. P_o = 1.1 kdyn; length = 1.13 cm; mass ~1 mg. Nominal resting sarcomere length, 2.4 μm.

[1]This variation is in agreement with Borejdo and Mason (1976) and is likely to be real, rather than due to translation of sarcomeres through the laser beam, for two reasons. Firstly, similar results have been obtained using markers rather than a laser (Steinen and Blange, 1981; Kobayashi and Sugi, 1982). Secondly, one may estimate the maximum errors due to translation as follows. Although a scan along the length of a bundle reveals resting sarcomere lengths that differ by perhaps 10%, over distances of 1–2 mm, the variation in sarcomere length is ~3%. For a real segmental length change of say 2% the maximum translation can be estimated as 0.02 × L_o or ~0.3 mm. For a laser beam covering 1.3 mm of the fiber, ~25% (that is 0.3/1.3) of the sarcomere population sampled by the beam might change during a contraction. Since local variation of sarcomere length is ~3%, at the point in the fiber farthest from the least compliant region, translation could account for an apparent sarcomere length shift of 0.25 × 3% = 0.75%. The average error for all locations along the fiber would be half of this, or 0.4%. This would change our estimate of the series compliance by only 20%.

0.82 ± 0.07 SEM (N = 5, range 0.59–0.98) of its tetanic value, at 26°C stiffness reached an average of only 0.63 ± 0.04 (N = 3) its tetanic value. At the peak of the twitch, P/P_0 was typically 0.68 ± 0.06 at 6°C and 0.32 ± 0.06 at 26°C. Force and stiffness appear to peak at approximately the same time although because of the increasing longitudinal nonuniformity near the peak of the twitch (see Fig. 5), it is difficult to be certain of the significance of this result.

Declining Phase of the Twitch

In Fig. 4, force relaxes more quickly than stiffness during the declining phase of the twitch. However, because the muscle bundle preparation is exceedingly longitudinally nonuniform during this phase of the twitch, interpretation of this portion of the records is difficult. Huxley and Simmons (1970) found that relaxation of a tetanus (0°C) of a single skeletal muscle fiber could be divided into two phases. During approximately the first one-third of relaxation the sarcomeres were relatively uniform longitudinally; it was only during the last two-thirds of relaxation that some portions of the fiber were stretched while others shortened. Fig. 7 shows that a phenomenon similar to that reported by Huxley and Simmons (1970) exists in semitendinosus bundles both at 6 and 26°C. For each record sarcomere length remains constant for some time after the force starts to fall. Fig. 8, which displays the relative stiffness and force changes during relaxation of a tetanus, shows that as in a twitch, stiffness decays less rapidly than force during relaxation. This is true both during the period when sarcomere length is constant as well as afterward.

Transmission Time as a Measure of Muscle Stiffness and Cross-Bridge Number

Fig. 9 shows the stiffness and force of a frog semitendinosus bundle at rest and during tetanic stimulation at different sarcomere lengths. It is seen that active force and active stiffness are both roughly proportional to the amount of overlap between the thick and thin filaments. In several experiments, relative stiffness seemed to be higher

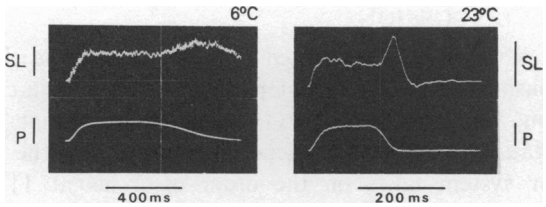

FIGURE 7 Sarcomere length change during a tetanus at 6° and 23°C in tendon-clamped semitendinosus bundles. *Upper curves*, sarcomere length (*SL*) change (shortening, upward). *Lower curves*, tetanic force (*P*). Vertical calibration bars near each record represent either 1.0 kdyn of force or 22 nm/half-sarcomere of shortening. Horizontal bars represent 400 ms at 6°C or 200 ms at 23°C. Note that during relaxation the average sarcomere length does not change at the point of observation (near middle of preparation) until the time indicated by the thin vertical line when force has already significantly dropped.

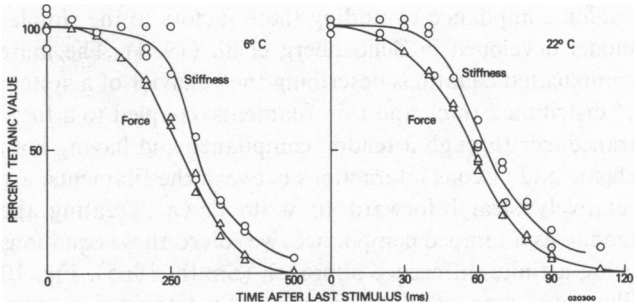

FIGURE 8 Force and stiffness during relaxation of a tetanus at 6° and 22°C. Last stimulus applied at time equals zero. *Ordinate*, percent of tetanic value of force (△) or stiffness (○). *Abscissa*, time (ms). Experiment 020300. P_0 = 10.0 kdyn at 6°C; P_0 = 12.0 kdyn at 22°C; mass equals 8.8 mg; length equals 1.4 cm; sarcomere length equals 2.2 μm.

than relative force at intermediate sarcomere lengths but the statistical significance of this could not be shown.

The rough parallelism between active force, active stiffness, and filament overlap suggests that the increased stiffness measured in the activated muscle using the transmission time technique is closely related to the number of attached cross bridges. This extent of agreement is actually somewhat surprising considering the approximations inherent in applying the technique. Both tendon compliance and muscle viscosity are ignored. Mechanical disturbances in a muscle can be transmitted not only by springlike links between the filaments but by viscous forces as well. If the effect of viscous forces is large in a resting muscle, it is not appropriate to subtract the resting "stiffness" from the activated stiffness.

One can get an estimate of the effects of viscosity and

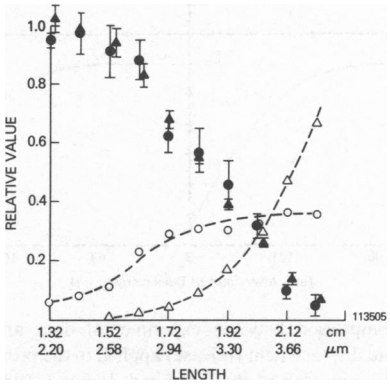

FIGURE 9 Relative tetanic stiffness and force vs. muscle length. *Upper abscissa*, muscle length in centimeters. *Lower abscissa*, resting sarcomere length at one location near the center of muscle bundle (microns). Open symbols: resting tension (△) and stiffness (○). Filled symbols: total tension in activated muscle minus resting tension (▲) or total stiffness in activated muscle minus resting stiffness (●). Vertical bars show standard error of the mean (SEM). Each point is the average of 2–5 measurements. Fiber bundle stimulated once every 3 min. Values were calculated relative to the average of the nearest pre- and post-record control. Experiment terminated when control decreased to 80%. For purposes of display a few of the force data points, obtained at the same sarcomere length as the stiffness data points, have been laterally displaced to show the SEM. Fiber bundle 113505; P_0 = 12.5 kdyn; mass equals 10.3 mg.

tendon compliance by adding these factors to the simpler model developed in Schoenberg et al. (1974). The more complicated equations describing the behavior of a system of distributed thick and thin filaments, coupled to a force transducer through a tendon compliance and having both elastic and viscous interactions between the filaments, are relatively straightforward to write down. Treating the tendon as a lumped compliance, we solved these equations using a finite-difference approach (Smith, 1965). Fig. 10 illustrates data obtained from a fully tetanized muscle, compared with theoretical predictions of different models. Fig. 10 *A* compares the displacement used in the computations, ($u = \beta t^3$), with the actual displacement record. The two agree quite well. (All fitting of parameters was done on a PDP-10 computer [Digital Equipment Corp., Marlboro, MA] using a nonlinear curve fitting routine based upon Marquadt's compromise.) Fig. 10 *B* shows a comparison

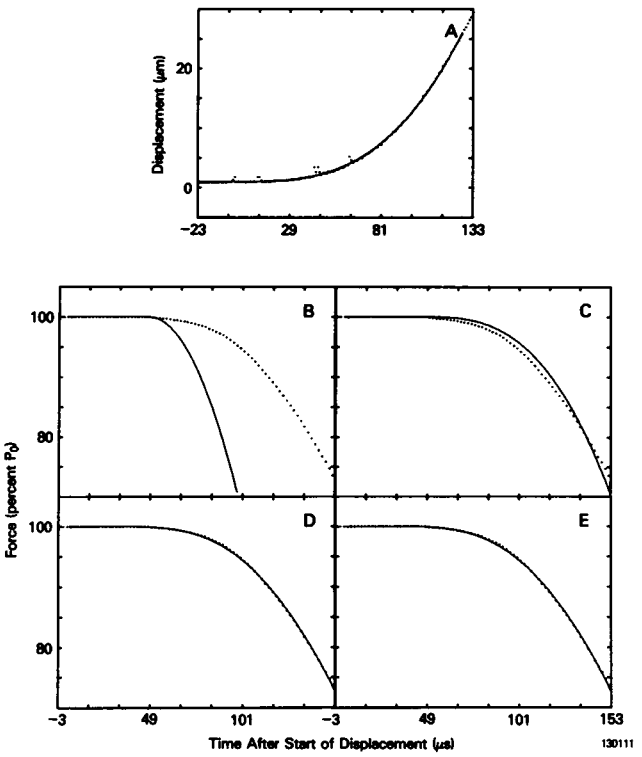

FIGURE 10 Comparison between experimental data and theoretical models for a rapid displacement (release) applied to the proximal end of a muscle with force recorded at the distal end. Points (·), digitized data. Solid lines (——), theoretical curves. (*A*) Displacement record at proximal end with best least-squares fit to relationship $u = a_o + \beta t^3$. β was found to be 1.225×10^{-9} cm · μs^{-3}. *B–E* Comparison of experimental force record with predictions for various model parameters. (*B*) Muscle stiffness, ξ_m, equals 463, determined using the assumptions of Schoenberg et al. (1974) (tendon stiffness, $\xi_t = \infty$; coefficient of viscosity, $\eta = [\Delta P/P_o]/[L^{-1}\, du/dt] = 0$). (*C*) Muscle stiffness, ξ_m as in *B*, but tendon stiffness, ξ_t, determined by best least-squares fit, equaling 8.6 (length of tendon divided by length of muscle, $L_t/L_m = 0.05$; $\eta = 0$). (*D*) $\xi_m = 910$, $\xi_t = 5.5$, both determined by least-squares curve fit ($L_t/L_m = 0.05$; $\eta = 0$). *E* Like *D*, except viscous coefficient, $\eta = 0.001$ s. From least-squares fit, $\xi_m = 828$, $\xi_t = 5.6$ ($L_t/L_m = 0.05$). Experiment 130111, $P_o = 1.84$ Mdyn/cm^2, $L_m = 1.4$ cm.

between the experimental and predicted force records when the stiffness is determined using the assumptions in Schoenberg et al. (1974), with no allowance made for tendon compliance. The fit is clearly quite poor. Retaining this value for muscle stiffness but allowing tendon compliance greatly improves the fit (Fig. 10 *C*). The fit can be further improved by allowing the curve fitting routine to select both muscle and tendon stiffness in fitting the curves (Fig. 10 *D*). In this case the muscle stiffness selected by the curve-fitting routine is roughly twice that determined using the assumptions of Schoenberg et al. (1974) and about three times the value reported by Ford et al. (1977). (If y_o is the compliance in nanometer/half sarcomere, the nondimensional stiffness, ξ_m, is $1{,}100/y_o$.) This very large discrepancy is most likely due to the fact that the value of muscle stiffness is not very well determined by the fit (slight variations in either the data or the value of muscle viscosity or tendon stiffness give large variations in ξ_m) and furthermore, ξ_m is probably not constant, as assumed here, for the 100–200-μs interval fitted in Fig. 10 (Ford et al., 1981). This means that while the above model is useful for illustrating some of the problems inherent in trying to obtain absolute values of stiffness using transmission time, fitting the model to the data does not offer a way around these problems. Finally, Fig. 10 *E* shows that including in the theoretical predictions that amount of viscosity that we measured in the resting fiber using the method of Ford et al. (1977) does not have a great effect. We include this computation simply for completeness as Ford et al. (1977) did not find evidence for this amount of viscosity in the fully tetanized fiber.

The above computations make clear that because of the complications of tendon compliance, it is difficult to obtain absolute values for muscle stiffness with the transmission time technique.[2] One may also use the above model to estimate the error in relative stiffness measurements of the type presented in this paper. Assuming that the tendon compliance is exponential, computations of the type shown in Fig. 10 suggest that relative stiffnesses in the range of 1/2–1/4 the isometric stiffness, S_o, would be overestimated by ~0.06 S_o. This applies to both Fig. 4 and Fig. 9.

DISCUSSION

Much work has been devoted to working out the time relationships of the various steps involved in muscle contraction. Gonzalez-Serratos (1971) has shown that the propagation of electrical depolarization down the T-tubular system takes on the order of 2 ms at 11°C. Measuring the time course of the intracellular calcium rise

[2]Although the transmission time technique would, as suggested by Schoenberg et al. (1974) greatly minimize the effect of tendon compliance when the tendon compliance is comparable with or less than the muscle compliance, Fig. 10 suggests that the tendon compliance is quite a bit more than the muscle compliance. (Because tendon stiffness is expressed per muscle length, the appropriate values of compliance to compare are ξ_m^{-1} and $\xi_t^{-1}[L_t/L_m]$.)

has been somewhat more difficult. Ashley and Ridgeway (1972) and Blinks et al. (1978) have shown that in aequorin loaded fibers, upon electrical stimulation, the time course of the light signal seemed to be faster than the force time course. However, as Blinks et al. (1978) point out, aequorin luminescence is unlikely to be a good measure of intracellular Ca^{2+} during the rising phase of a twitch. Metallochromic dyes are thought to be better indicators of rapid intracellular calcium transients (Baylor et al., 1982), although, because of sensitivity to movement artifacts, reliable data can only be obtained under conditions where contraction is suppressed. When contraction is suppressed by extending a semitendinosus muscle fiber to sarcomere length 3.7 μm, these dyes indicate that, at 16°C, intracellular Ca^{2+} concentration has already peaked and is starting to decline by ~10 ms (Baylor et al., 1982). If the same is true at a sarcomere length of 2.3 μm, then the rise of intracellular Ca^{2+} peaks well before the peak of force and stiffness.

The reason for the slower time course of stiffness relative to the intracellular Ca^{2+} signal is unclear. It is unlikely to be due to diffusional delay (Close, 1981). The slow rise in stiffness might be due to the time necessary for Ca^{2+} binding to troponin, the time necessary for a conformational change of troponin or tropomyosin, or the time necessary for a slow biochemical step (which could be the attachment step or a subsequent step necessary for the appearance of stiffness). Another possibility is that the rise in stiffness is delayed because the number of attached stiff cross bridges is decreased as a result of sarcomere shortening following activation. This would happen if the number of attached stiff bridges goes down with increased velocity of shortening as predicted by the model of A. F. Huxley (1957).

Most cross-bridge models also predict that sarcomere shortening will cause force development to be delayed. The exact lag between the rise of stiffness and the rise of force for a given amount of series compliance is very model dependent. As a frame of reference, the lag between stiffness and force predicted by the Huxley (1957) model parameters for the amount of series compliance seen in our experiments is only about one-half as large as the lag between stiffness and force shown in Fig. 4 (M. Schoenberg, unpublished computations).[3] One possible explanation for this discrepancy is that there is less change in the number of cross bridges as a function of velocity than predicted by this model. However, it is very difficult to state with certainty what effect multiple attached states (Huxley and Simmons, 1971), reverse rate constants (Hill et al., 1975), and pre-steady state transients (Civan and Podolsky, 1966; Huxley and Simmons, 1972), or other ways of modeling noninstantaneous activation might have upon the predicted relationship between stiffness and force. With regard to the lag between stiffness and force, changes in several of the low angle x-ray reflections also precede force following stimulation (Huxley, 1979; Matsubara and Yagi, 1978; Huxley et al., 1982).

Fig. 4 shows that although during the rising phase stiffness precedes force, during the falling phase of the twitch, stiffness falls more slowly than force. To ascertain whether this is an artifact caused by the extreme longitudinal nonuniformity of our preparations during the relaxation phase of the twitch, we measured the fall of stiffness and force early during relaxation of tetanus where the sarcomere length could be shown to be relatively constant (Fig. 7). Fig. 8 illustrates that stiffness here too falls less rapidly than force. This observation might be explained in terms of a higher rate constant for dissociation of high-force producing cross bridges than for low-force cross bridges. Kawai and Brandt (1976) have suggested differential rate constants for high- and low-force producing bridges, at least in rigor, although their effect is in the opposite direction from that required here. Clearly, many other factors could influence the decay of force and stiffness following cessation of stimulation, but again it is of interest to note that the intensity of certain x-ray reflections also return to their resting values more slowly than force following tetanic stimulation (H. E. Huxley, 1972; Yagi et al., 1977; Huxley et al., 1982).

One should be cautious about overinterpreting the precise values for the lags between stiffness and force. As we have pointed out, tendon compliance can cause some overestimation of the relative stiffness, although this is likely (see last section of Results), to account for only some of the lag shown in Fig. 4. Another concern about overinterpreting our value for the precise lag between stiffness and force is that if individual fibers in the multifiber preparation behave very differently, the stiffness measured using transmission time might reflect that of the stiffest fibers only, whereas the force measured would reflect that exerted by all the fibers. However, the similarity of our results during the rising phase, using bundles, and the results of Bressler and Clinch (1974) using whole muscle and Cecchi et al. (1982) using single fibers, suggest that this is not a serious problem.

The assumption that cross-bridges can be described by a frequency independent stiffness is questioned by the finding of Kawai et al. (1977) that over certain frequency ranges the stiffness of muscle is a complex quantity, having a real and an imaginary (i.e., frequency dependent) com-

[3]Activation was modeled by allowing the total number of cross bridges that could potentially make to be a linear function of time. It was necessary to explicitly compute the cross-bridge response since the relationships between sarcomere shortening and force or cross-bridge number in the nonsteady state are different from the relationships during steady state shortening (Civan and Podolsky, 1966). Since the Huxley model (1957) does not give rate constants necessary to compute the behavior of lengthening muscle, the model can only be compared with the behavior of the regions of the muscle that showed shortening following stimulation. In theory, the same calculations could also be done by separately comparing the lengthening segments with a model having appropriate constants for a lengthening muscle.

ponent. The frequencies they studied were below the frequencies involved in the transmission time measurement. Recent results of Cecchi et al. (1982), that show a constant stiffness at 4 and 7 kHz, suggest that at higher frequencies the stiffness of the fully activated muscle is not extremely frequency dependent.

It is appropriate to ask whether one may describe propagation through muscle bundles simply in terms of a longitudinal elastic modulus or whether bulk propagation effects also need to be considered. For an isotropic viscoelastic material, the former approach is strictly valid only when the ratios of the preparation radius to the preparation length and also to the wavelength of the propagated signal are $< \sim 0.2$ (Kolsky, 1963). Since the foot of the propagated disturbance that we analyze is propagating at ~200 m/s and has a duration of 15 μs (see Schoenberg et al., 1974, p. 637), the above constraints require that the diameter of our bundles be <1.2 mm. Generally the fiber bundle diameters were 1 mm or less so this constraint was met.

Relationship to Other Types of Mechanical Studies

Hill (1951) and Abbott and Ritchie (1951) showed that the ability to shorten at near maximal values is achieved quite rapidly, in 20–25 ms near 0°C. This is reasonable because while stiffness and the ability to support tension presumably depend upon cross-bridge number, the ability to shorten at zero load may reflect only cross-bridge cycling rate and not require complete activation of all the parallel contractile elements. The ability of a muscle to support full isometric tension upon stretch appears (Hill, 1970) some 50 ms after activation at 0°C. This is also compatible with our findings when one considers that stretch experiments of the isometric muscle (Katz, 1939; Flitney et al., 1976) suggest that cross bridges may be capable of supporting tension upon stretch some 60% greater than isometric tension. In this case, a fraction of only 1/1.6 of the cross bridges could conceivably support full isometric tension during stretch experiments and if stiffness reflects cross-bridge number, then our stiffness measurements suggest that this fraction of cross bridges exists within 40 ms of the twitch stimulus at 6°C. Our stiffness measurements also correlate nicely with the findings of Cecchi et al. (1978) who found that the ability of a muscle to shorten against a load, which should depend upon cross-bridge number, reaches its tetanic value after ~100 ms at 4°C. This agrees with the 100 ms taken for practically full tetanic stiffness to develop at 6°C as seen in Fig. 4.

The authors wish to acknowledge many helpful discussions with Drs. Richard J. Podolsky, Evan Eisenberg, and Elizabeth Stephenson. The authors also thank Acoustic Research (Norwood, MA) for providing the speaker coil assemblies used in the experiments.

Received for publication 16 November 1982 and in final form 17 August 1983.

REFERENCES

Abbott, B. C., and J. M. Ritchie. 1951. The onset of shortening in striated muscle. *J. Physiol.* (*Lond.*). 113:336–345.

Ashley, C. C., and E. B. Ridgway. 1972. On the relationships between membrane potential, calcium transient, and tension in single barnacle muscle fibers. *J. Physiol.* (*Lond.*). 209:105–130.

Baylor, S. M., W. K. Chandler, and M. W. Marshall. 1982. Use of metallochromic dyes to measure changes in myoplasmic calcium during activity in frog skeletal muscle fibres. *J. Physiol.* (*Lond.*). 331:139–177.

Blinks, J. R., R. Rudel, and S. R. Taylor. 1978. Calcium transients in isolated amphibian skeletal muscle fibers: detection with aequorin. *J. Physiol.* (*Lond.*). 277:291–323.

Borejdo, J., and P. Mason. 1976. Sarcomere length changes during stimulation in frog semitendinosus muscle. *J. Mechanochem. Cell Motil.* 3:155–161.

Bressler, B. H., and N. F. Clinch. 1974. The compliance of contracting skeletal muscle. *J. Physiol.* (*Lond.*). 237:477–493.

Cecchi, G., F. Colomo, and V. Lombardi. 1978. Force-velocity relation in normal and nitrate-treated frog single muscle fibres during rise of tension in an isometric tetanus. *J. Physiol.* (*Lond.*). 285:257–273.

Cecchi, G., P. J. Griffiths, and S. Taylor. 1982. Muscular contraction: kinetics of crossbridge attachment studied by high-frequency stiffness measurements. *Science* (*Wash., DC.*). 217:70–72.

Civan, M. M., and R. J. Podolsky. 1966. Contraction kinetics of striated muscle fibres following quick changes in load. *J. Physiol.* (*Lond.*). 184:511–534.

Cleworth, D. R., and K. A. P. Edman. 1972. Changes in sarcomere length during isometric tension development in frog skeletal muscle. *J. Physiol.* (*Lond.*). 222:1–17.

Close, R. I. 1981. Activation delays in frog twitch muscle fibres. *J. Physiol.* (*Lond.*). 313:81–100.

De Barr, A. E. 1962. Automatic Control. Chapman and Hall, Ltd. London. 106–109.

Flitney, F. W., D. G. Hirst, and D. A. Jones. 1976. Effects of temperature and velocity of stretch on the maximum tension borne by the sarcomeres in contracting muscle. *J. Physiol.* (*Lond.*). 256:127–128P.

Ford, L. E., A. F. Huxley, and R. M. Simmons. 1977. Tension responses to sudden length change in stimulated frog muscle fibres near slack length. *J. Physiol.* (*Lond.*). 269:441–515.

Ford, L. E., A. F. Huxley, and R. M. Simmons. 1981. The relationship between stiffness and filament overlap in stimulated frog muscle fibres. *J. Physiol.* (*Lond.*). 311:219–249.

Gonzalez-Serratos, H. 1971. Inward spread of activation in vertebrate muscle fibres. *J. Physiol.* (*Lond.*). 212:777–800.

Hill, A. V. 1951. The transition from rest to full activity in muscle: the velocity of shortening. *Proc. Roy. Soc. Ser. B.* 138:329–338.

Hill, A. V. 1970. First and last experiments in muscle mechanics. Cambridge University Press, Cambridge, England. 1–141.

Hill, D. K. 1968. Tension due to interaction between the sliding filaments in resting striated muscle: the effect of stimulation. *J. Physiol.* (*Lond.*). 199:637–684.

Hill, T. L., E. Eisenberg, Y. Chen, and R. J. Podolsky. 1975. Some self-consistent two-state sliding filament models of muscle contraction. *Biophys. J.* 15:335–372.

Huxley, A. F. 1957. Muscle structure and theories of contraction. *Prog. Biophys. Biophys. Chem.* 7:255–318.

Huxley, A. F., and R. M. Simmons. 1970. Rapid 'give', and the tension 'shoulder' in the relaxation of frog muscle fibres. *J. Physiol.* (*Lond.*). 210:32–33P.

Huxley, A. F., and R. M. Simmons. 1971. Proposed mechanism of force generation in striated muscle. *Nature* (*Lond.*). 233:533–538.

Huxley, A. F., and R. M. Simmons. 1972. Mechanical transients, and the origin of muscular force. *Cold Spring Harbor Symp. Quant. Biol.* 37:669–680.

Huxley, H. E. 1972. Structural changes in the actin- and myosin-

containing filaments during contraction. *Cold Spring Harbor Symp. Quant. Biol.* 37:361–376.

Huxley, H. E. 1979. Time-resolved x-ray diffraction studies on muscle. *In* Cross-bridge mechanism in muscle contraction. H. Sugi and G. Pollack, editors. University Park Press, Baltimore. 389–405.

Huxley, H. E., A. R. Faruqi, M. Kress, J. Bordas, and M. H. J. Koch. 1982. Time-resolved x-ray diffraction studies of the myosin layer-line reflections during contraction. *J. Mol. Biol.* 158:637–684.

Jewell, B. R., and D. R. Wilkie. 1958. An analysis of the mechanical components in frog's striated muscle. *J. Physiol.* (*Lond.*). 143:515–540.

Katz, B. 1939. The relation between force and speed in muscular contraction. *J. Physiol.* (*Lond.*). 96:45–64.

Kawai, M., and P. W. Brandt. 1976. Two rigor states in skinned crayfish single muscle fibers. *J. Gen. Physiol.* 68:267–280.

Kawai, M., P. W. Brandt, and M. Orentlicher. 1977. Dependence of energy transduction in intact muscle fibers on the time in tension. *Biophys. J.* 18:161–172.

Kobayashi, T., and H. Sugi. 1982. Segmental length changes in stimulated frog sartorius muscle during dynamic mechanical responses. *Jap. J. Physiol.* 32:817–830.

Kolsky, H. 1963. Stress waves in solids. Dover Publications, Inc., New York.

Matsubara, I., and N. Yagi. 1978. A time-resolved x-ray diffraction study of muscle during twitch. *J. Physiol.* (*Lond.*). 278:297–307.

Schoenberg, M., J. B. Wells, and R. J. Podolsky. 1974. Muscle compliance, and the longitudinal transmission of mechanical impulses. *J. Gen. Physiol.* 64:623–642.

Smith, G. D. 1965. Numerical solution of partial differential equations. Oxford University Press, New York. 1–97.

Steinen, G. J. M., and T. Blange. 1981. Local movement in stimulated sartorius muscle. *J. Gen. Physiol.* 78:151–170.

Yagi, N., M. H. Ito, H. Nakajima, T. Izumi, and I. Matsubara. 1977. Return of myosin heads to thick filaments after muscle contraction. *Science* (*Wash., DC.*). 197:685–587.